applied optics

Noniterative multiplane holographic projection

ALEJANDRO VELEZ-ZEA[1,*] AND ROBERTO TORROBA[1,2]

[1]Centro de Investigaciones Ópticas (CONICET La Plata- CIC-UNLP), P.O. Box 3, C.P 1897 La Plata, Argentina
[2]UIDET OPTIMO, Departamento de Ciencias Básicas, Facultad de Ingeniería, Universidad Nacional de La Plata, La Plata, Argentina
*Corresponding author: alejandrov@ciop.unlp.edu.ar

Received 20 February 2020; revised 12 April 2020; accepted 14 April 2020; posted 14 April 2020 (Doc. ID 390707); published 7 May 2020

In this paper, we introduce a mixed complex and phase-only constraint for noniterative computer generation of phase-only holograms from multiplane intensity distributions. We are able to reproduce three-dimensional intensity distributions with the same number of planes achieved with the Gerchberg–Saxton (GS) algorithm; at the same time, we maintain the fast computation time of a noniterative method. In this way, we enable the possibility of multiplane light field control in dynamic applications. We show numerical results for three- and eight-plane holograms, for different interplane distances—using either the same or different amplitude constraints in each plane. In all of these tests, our method results in a comparable or better reconstruction quality than the GS algorithm, while achieving a significant decrease in computing time. Finally, we experimentally demonstrate the capability of our proposal to achieve multiplane holographic projection.

https://doi.org/10.1364/AO.390707

1. INTRODUCTION

Modern phase-only spatial light modulators (SLM) allow for the precise control of light fields, enabling a broad range of applications that were previously unfeasible. Those applications include super-resolution microscopy [1,2], optical encryption [3,4], optical trapping [5,6], and neuronal photostimulation [7]. All of these applications have shown tremendous potential for pushing state-of-the-art optical diagnostic, metrology, and characterization techniques forward.

However, the capability to precisely modulate the phase of the optical field is only one of the challenges posed by these applications because most of them require light field control, not only in a plane, but also in a three-dimensional (3D) region of space. As a result, the target light field in a 3D volume must be first codified into a single, 2D phase-only function.

Many techniques have been developed under the field of computer-generated holography (CGH). In particular, CGH techniques result in a 2D function (hologram) that reproduces a target optical field. There are different methods, depending on the features of the target. Some CGH techniques are well suited to reproduce single 2D targets, while others are better optimized for 3D distributions. The type of hologram to be generated also must be taken into account, with some methods producing complex valued holograms, while others result in either amplitude-only or phase-only holograms.

Advances in phase-only SLM and the importance of the aforementioned applications, have created CGH methods to produce phase-only holograms of special interest. For instance, in optical trapping, a single phase-only hologram must be able to generate intensity spots to confine multiple particles in a 3D volume. Likewise, in the case of holographic displays, it may be necessary to codify multiple objects in different planes.

The methods to generate these holograms can be classified as either iterative or noniterative, depending on the algorithm used. Amongst the iterative methods, we find the original Gerchberg–Saxton (GS) algorithm [8] and its variations, often called alternative projection algorithms [9,10]. In these methods, the constraints on the light field in two or more planes are known (for example, in a plane containing the object and in the hologram plane). The field is transformed back and forth between each plane, and the amplitude of the result replaced by the corresponding constraint. This process is repeated until the final result satisfies some quality metric. Other iterative methods include the use of gradient descent optimization [11], nonconvex optimization [12], or double constrains [13], to name a few. Iterative methods generally produce high-quality holograms; however, the need for multiple iterations makes dynamic applications difficult.

On the other hand, noniterative methods take advantage of certain light propagation features to generate holograms in a single step, without the need for multiple back and forth transforms or other optimization procedures. One of the most straightforward noniterative techniques is the random superposition method. In this method, the target amplitude in each plane is multiplied by a random phase and then backpropagated to the hologram plane [14]. The phase resulting from the superposition of the fields from all planes will be the final phase hologram. Despite its simplicity, this method is limited both

in the reconstruction quality and in the number of planes that can be reproduced from a single hologram. Other noniterative methods codify the complex hologram into two phase functions [15–17], or use patterned phase masks [18], where each constrain is multiplied by a tiled random phase. The periodicity of the tiled random phase leads to an increase in the reconstruction quality.

More recently, hybrid methods have been developed, where random phases are optimized using prior knowledge about the optical system [19,20]. These optimized random phases are then used for noniterative hologram generation. In this way, the reconstruction quality can be increased, while the computation speed remains lower than in standard iterative algorithms.

Inspired in these contributions, we now introduce what we believe is a new, noniterative method to generate multiplane holograms. Our proposal allows for the reproduction of 3D intensity distributions with a number of planes, comparable to the GS algorithm. At the same time, we maintain the fast computation time of a noniterative method, enabling the possibility of multiplane light field control in dynamic applications. We use a mixed complex and phase-only constrain in each plane during hologram generation to achieve this control. Additionally, we demonstrate the reconstruction of multiplane intensity distributions, and include comparisons to the conventional GS algorithm. Finally, we perform the experimental optical reconstruction of the holograms generated with our proposal by means of a phase-only SLM.

2. NONITERATIVE MULTIPLANE HOLOGRAM GENERATION

We now proceed to introduce our method for noniterative multiplane hologram (NIMH) generation. Our objective is to obtain a single-phase hologram that results in a given multiplane intensity distribution after reconstruction, as shown in Fig. 1.

There are several iterative approaches that can achieve this kind of multiplane hologram. The most straightforward of these techniques is the GS algorithm. In this method, an initial random phase is propagated to the first plane in the target intensity distribution volume. Then, the resulting amplitude is replaced with the target amplitude, preserving the phase. The complex field is then propagated to the next plane, where the process is repeated. This is done for each plane of the target intensity distribution. After reaching the final plane, the procedure is carried out backwards. Finally, once the hologram plane is reached, the amplitude is again discarded and replaced by a constant. This entire procedure is repeated and, in each iteration, the phase in the hologram plane will reproduce a closer approximation to the target intensity distribution.

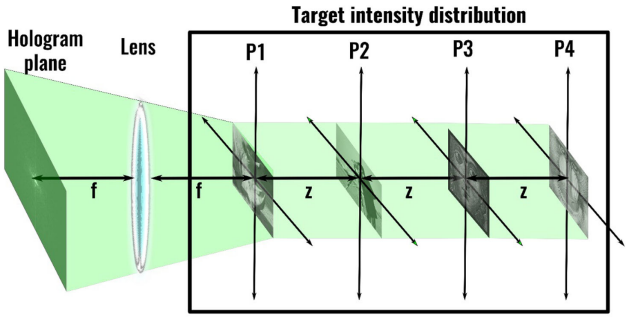

Fig. 1. Scheme of the reconstruction of a multiplane hologram. P: target plane, z: interplane distance, f: lens focal length.

As can be inferred from the description of the method, this approach is computationally intensive. Furthermore, it is prone to stagnation, and the accuracy of the achieved intensity distribution will diminish as the number of planes is increased.

The stagnation and low quality of the result can be partially explained because the amplitude target in each plane imposes a constrain not only in that plane, but also in the rest of the planes of the intensity distribution. Piestun *et al.* demonstrated a way to solve this issue: relaxing the amplitude constraints in each plane by giving a small, nonzero value to the zero-intensity regions in each plane [21]. In this way, they were able to reproduce a two-plane intensity distribution from a single, low-resolution binary hologram.

Our proposal builds on the concept of relaxing the constraints. In particular, we perform the same basic procedure found in the first iteration of the GS algorithm. However, in each plane we set the complex field as a linear combination of the products of the full complex field and its phase-only part with the amplitude target. Additionally, we relax the amplitude constraint by using a small, nonzero value in the zero-intensity regions.

Thus, in plane i the complex field will be given by

$$F_i(v, w) = a_i(v, w)(C \cdot \mathrm{FrT}_z(F_{i-1}(v, w)) + (1 - C) \cdot \exp(j\phi_{i-1}(v, w))), \quad (1)$$

where FrT is the Fresnel transform with distance z, z is the distance between the plane i and $i - 1$, C is a constant that determines the weight of the complex and phase part, $a_i(v, w)$ is the amplitude constrain for that plane, and $\phi_{i-1}(v, w)$ is the phase of the Fresnel transform of the field in the previous plane.

Once the last plane is reached, the procedure is performed backward, with the field in each plane replaced by

$$F_i(v, w) = a_i(v, w)(C \cdot \mathrm{FrT}^{-1}{}_z(F_{i+1}(v, w)) + (1 - C) \cdot \exp(j\phi_{i+1}(v, w))), \quad (2)$$

where FrT^{-1} is the inverse Fresnel transform with distance z, and z is the distance between the plane i and $i + 1$. This procedure is done until the hologram plane is reached, where the amplitude is discarded and the remaining phase will become our hologram.

Using the factor C, we can control how the amplitude constraints from the rest of the planes affect the overall intensity distribution. A C factor of 0 means that our proposal will behave as a single iteration of the GS algorithm, returning a hologram with low accuracy after reconstruction. AC factor of 1 will result in heavy occlusion and cross-talk between the amplitude constrains of each plane, also resulting in very low-quality reproduction of the desired intensity distribution.

However, when C is set to 0.5, we give equal weight to both the full complex field and its phase-only component. In this case, we achieve a hologram that reproduces the target intensity distribution with improved accuracy, achieving similar results

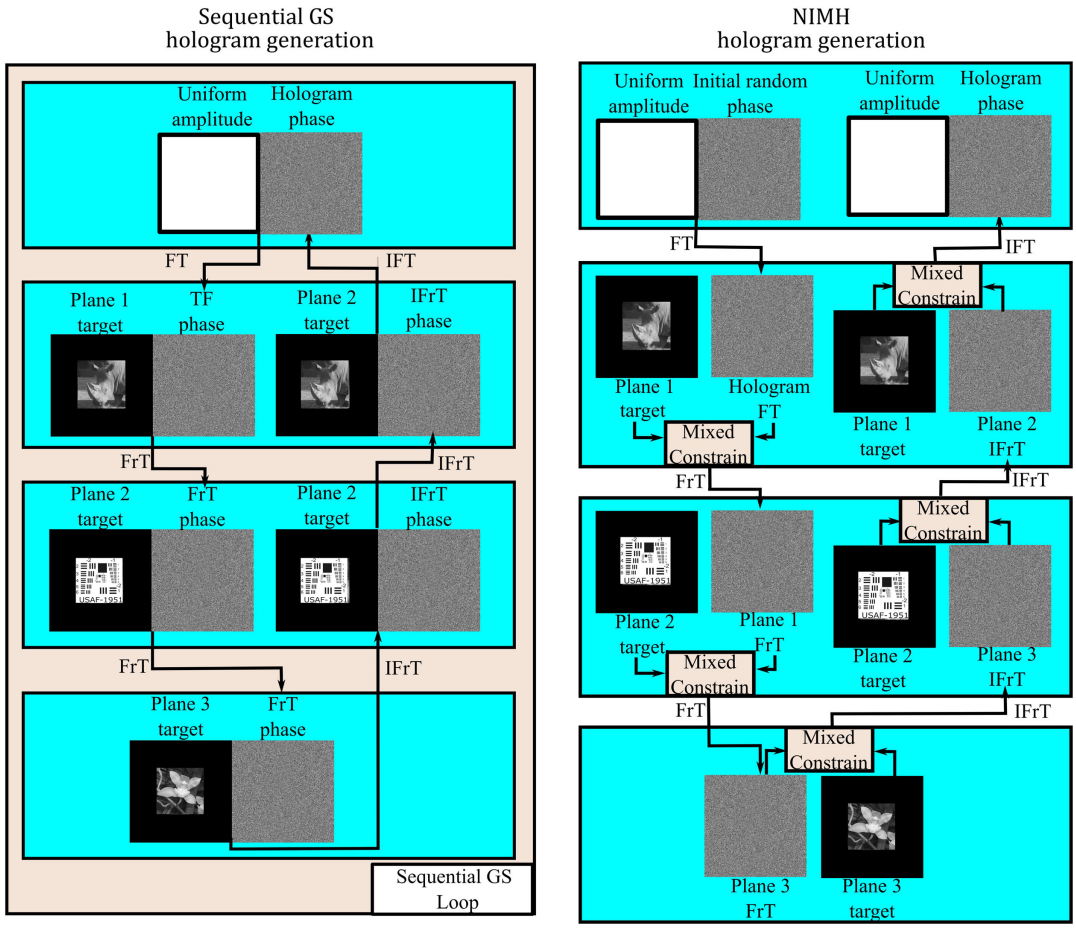

Fig. 2. Flowchart of the GS and NIMH methods for generation of three-plane holograms.

in a single step to hundreds of iterations of the conventional GS method.

In Fig. 2, we show a flowchart of both the sequential GS algorithm and the NIMH methods to generate a hologram corresponding to a three-plane intensity distribution. The mixed constrain block in the NIMH flowchart denotes the linear combination of the products of the full complex field and its phase-only part with the amplitude target. Unlike the GS algorithm, the NIMH method only requires a single pass forward and backward through all the planes in the intensity distribution. Additional loops will result in an increase of the cross-talk between planes, decreasing the quality of the result in the same way that using the higher values of the parameter C; thus our method is essentially noniterative. On the other hand, to achieve optimal results with the GS method, several iterations are required.

3. NUMERICAL RESULTS

We now proceed to numerically test our proposal and compare it to the results from the GS algorithm. First, we will test the effect of the parameter C in the reconstruction of a three-plane intensity distribution with both grayscale and binary amplitude targets. For this test, we set the interplane distance as 4 cm. The hologram resolution is 1920×1920 pixels, with a pixel size of 8 μm. The illumination wavelength is 532 nm. The amplitude constraints consist of images with a resolution of 1500×1500 pixels. To ensure the highest quality results for the GS algorithm, we applied 200 iterations. In general, between 20 and 50 iterations offers the best relation between quality and computing time for this algorithm, with further iterations resulting in comparatively small increases in quality.

As we can see from the results in Fig. 3, using our proposal with a C value of 0 results in very low quality in the reconstruction of plane 2, and especially in plane 3. On the other hand, with a C value of 1, there is strong cross-talk between planes, degrading the overall quality. However, a C value of 0.5 produces results that present a very strong similitude to the use of 200 iterations of the GS algorithm. To further verify the similitude between the NIMH method the GS algorithm, we show in Fig. 4 the cross-section of light propagation in the target intensity distribution volume.

As shown in this result, the NIMH generated with values of $C = 0.5$ [Fig. 4(b)] is very similar to the GS result [Fig. 4(d)], while with $C = 1$ [Fig. 4(c)] we obtain a strong concentration of energy in the center of the intensity distribution, and with $C = 0$ [Fig. 4(a)] we obtain smaller variations in the energy, due to the inadequate reproduction of the amplitude constraints. It can be appreciated in P2 of Fig. 4, where there is a low-intensity region that corresponds to the dark part of the USAF target used as amplitude constraint for that plane. That region shows low contrast in Fig. 4(a), compared to Figs. 4(b) and 4(d).

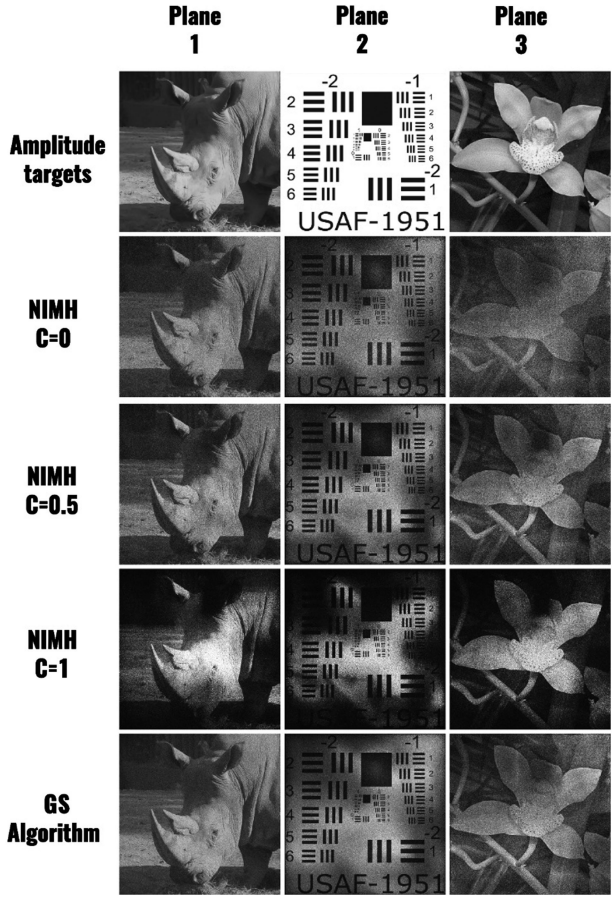

Fig. 3. Comparison between the reconstruction of GS-generated holograms and NIMH for different values of C.

Now that we have determined that a C value of 0.5 results in noniterative multiplane holograms with quality comparable to those obtained with the GS algorithm, we proceed to test the performance of our method using this value for different scenarios. First, we will test the effects of introducing additional planes to the target intensity distribution volume. For this test, we will generate a NIMH and a GS hologram with eight planes, using different images as amplitude constraints in each plane. The interplane distance was set at 4 cm.

As we can see from Fig. 5, in both the GS and the NIMH, the first planes present a relatively high reconstruction quality; nevertheless, the planes further away from the hologram suffer increasing degradation. In particular, the reconstruction in the eighth plane is unrecognizable in both methods. Despite this issue, the rest of the planes present very similar reconstruction quality, with the GS results having better quality for the first two planes and then being surpassed by the NIMH results for the remaining planes.

Another interesting application of multiplane holograms is reproducing the same target in different planes. This application can be useful to ensure extended focus distance in head-up displays. The effectiveness of our proposal in this scenario is verified by generating multiple holograms of the same three-plane intensity distributions, increasing the distance between each plane for each hologram. Then, we reconstructed the same plane for each hologram and calculated the structural similarity index (SSIM) of the result compared to the original amplitude target. We use the same amplitude target used in plane 4 of Fig. 5.

As we can see from Fig. 6, our method presents a slightly lower quality for the first two planes, but a very similar quality for the last plane. Furthermore, our method presents slower degradation than the GS algorithm as the interplane distance increases. We now proceed to test the behavior by increasing the number of planes with the same target in each plane, and calculating the SSIM between the original target as the reconstruction distance increases. For this test, the interplane distance was set at 4 cm.

In Fig. 7, we can see that the GS method has better quality for the first plane, but for the remaining planes our proposal has significantly increased quality. These results show that a greater depth of field can be maintained with higher quality when compared to the GS algorithm.

In Fig. 8 we show the reconstruction of each plane from the GS hologram and NIMH, confirming the behavior shown in the graph of Fig. 7.

We now proceed to show the computation time for both the NIMH and the GS results corresponding to the eight-plane intensity distribution shown in Fig. 5.

As we can see from Table 1, the NIMH method has a very similar computation time to a single iteration of the GS algorithm. The speed advantage of our method becomes evident the more iterations of the GS method are used. We achieved higher or comparable quality results with the NIMH compared to applying 200 iterations of the GS algorithm, which represents a nearly 110-fold increase in computing speed. For all numerical results in this work we used parallel computing with a NVIDA GTX 1060 TI GPU and an Intel i7-4770 K CPU. These results indicate that for all tested scenarios (including three or eight planes), different interplane distances, and using either the same or different amplitude constrains in each plane, our proposed method for noniterative hologram generation offers similar or better performance than the GS algorithm.

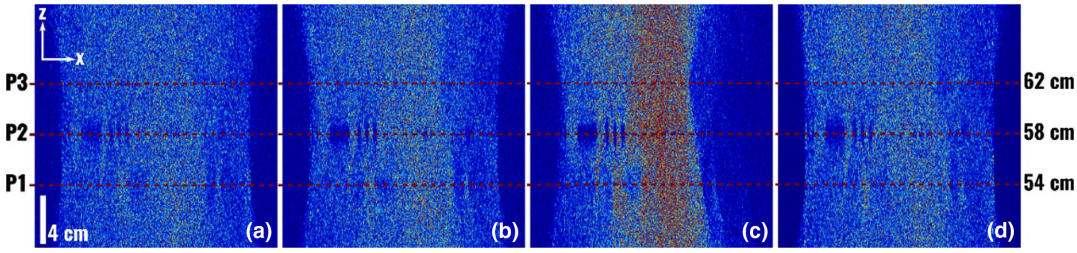

Fig. 4. Cross-section of light propagation from (a) NIMH with $C = 0$, (b) NIMH with $C = 0.5$, (c) NIMH with $C = 1$, and (d) hologram generated with 200 iterations of the GS algorithm.

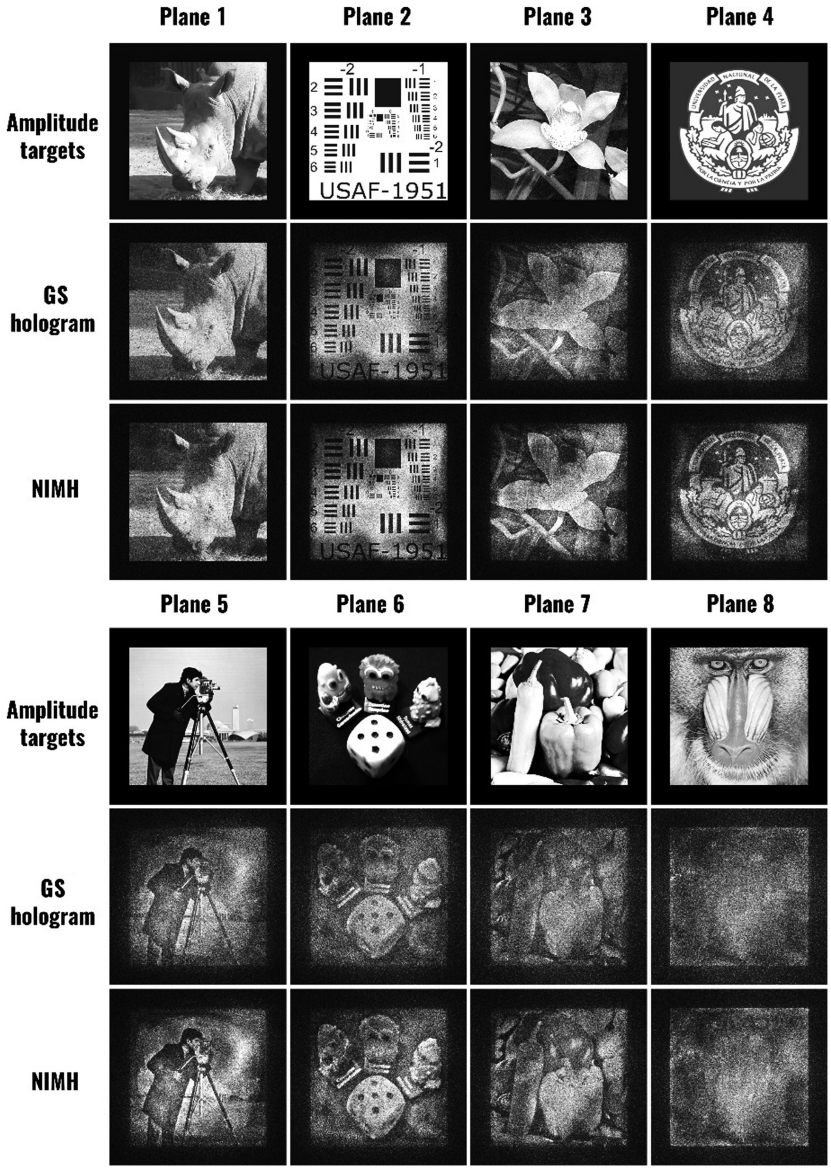

Fig. 5. Comparison between the reconstruction of an eight-plane intensity distribution from a GS-generated hologram and a NIMH.

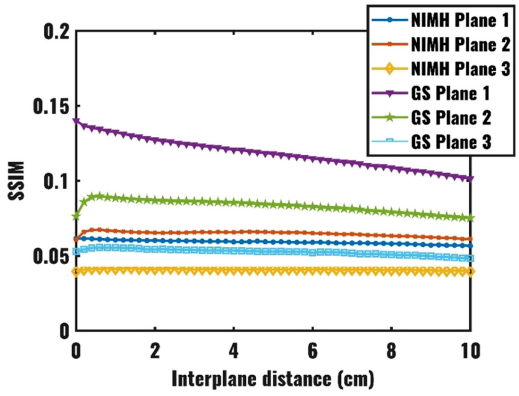

Fig. 6. SSIM of the different reconstruction planes from both NIMH and GS holograms as the interplane distance increases.

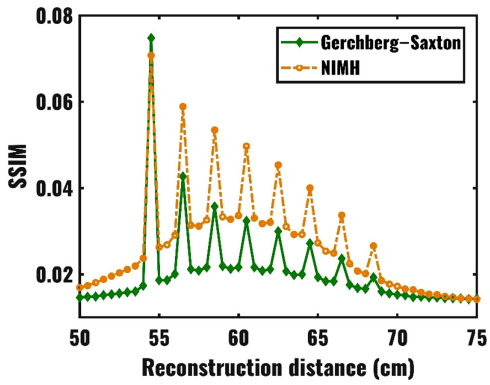

Fig. 7. SSIM of the different reconstruction planes for an eight-plane NIMH and GS hologram.

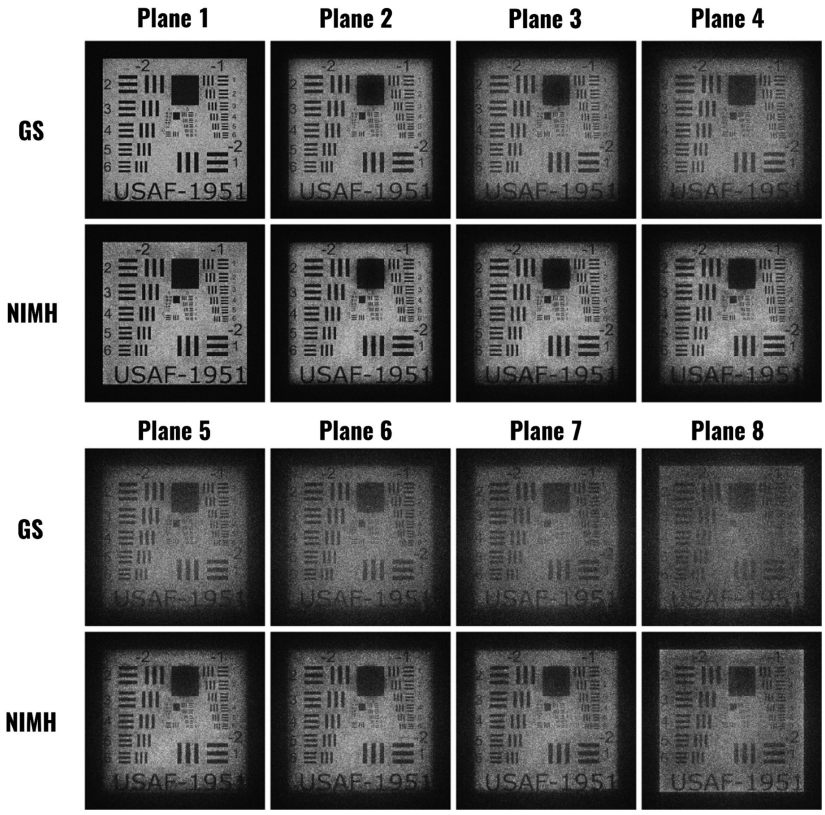

Fig. 8. Comparison between the reconstruction of an eight-plane intensity distribution from a GS-generated hologram and a NIMH when using the same target in all planes.

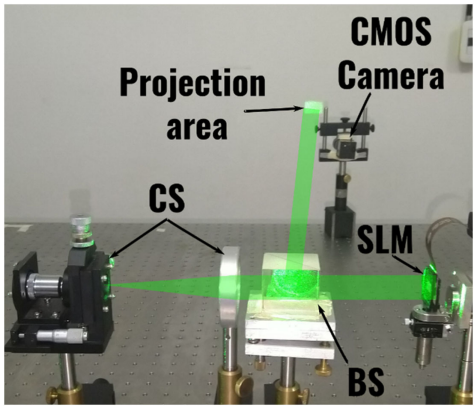

Fig. 9. Experimental setup for holographic projection using a LCOS-SLM. CS: collimation system, BS: beam splitter.

Table 1. Computation Time for Generation of a Hologram Corresponding to an Eight-Plane Intensity Distribution Using the NIMH and Different Number of Iterations of the GS Algorithm

Number of Iterations	NIMH Computation time (s)	GS Computation time (s)
1	1.612	1.478
10	–	9.142
20	–	19.049
200	—	178.582

4. EXPERIMENTAL RESULTS

We now proceed to experimentally test the capability of NIMH to reproduce multiple planes when used in a holographic projection system based on a phase-only liquid crystal on silicon (LCOS) SLM. For these tests, we implemented the experimental setup shown in Fig. 9.

In the experimental tests, we used the same NIMH and GS hologram as in the tests of Figs. 5 and 8. This corresponds to eight-plane intensity distributions. We tested holograms with different amplitude constraints in each plane as well as using the same amplitude constraint in all planes. The holograms had a resolution of 1920 × 1920 and were cut down to a resolution of 1920 × 1080 to match the SLM area. To avoid the effects of the zero order from the SLM, and to eliminate the need for lenses in the optical setup, we multiplied the holograms with a phase grating and a spherical phase. The frequency of the grating and the radius of the spherical phase allow us to control the position in 3D space of the reconstructed intensity distribution. The amplitude constraints are the input images shown in Fig. 5, with a resolution of 1200 × 1200 pixels each. The SLM used is a PLUTO-2-VIS-016 SLM with a resolution of 1920 × 1080 pixels and a pixel pitch of 8 μm. The illumination source is a Nd:YAG laser with an output power of 300 mW and a wavelength of 532 nm.

First, we test the performance of the multiplane holograms with different amplitude constraints. As we can see in Fig. 10,

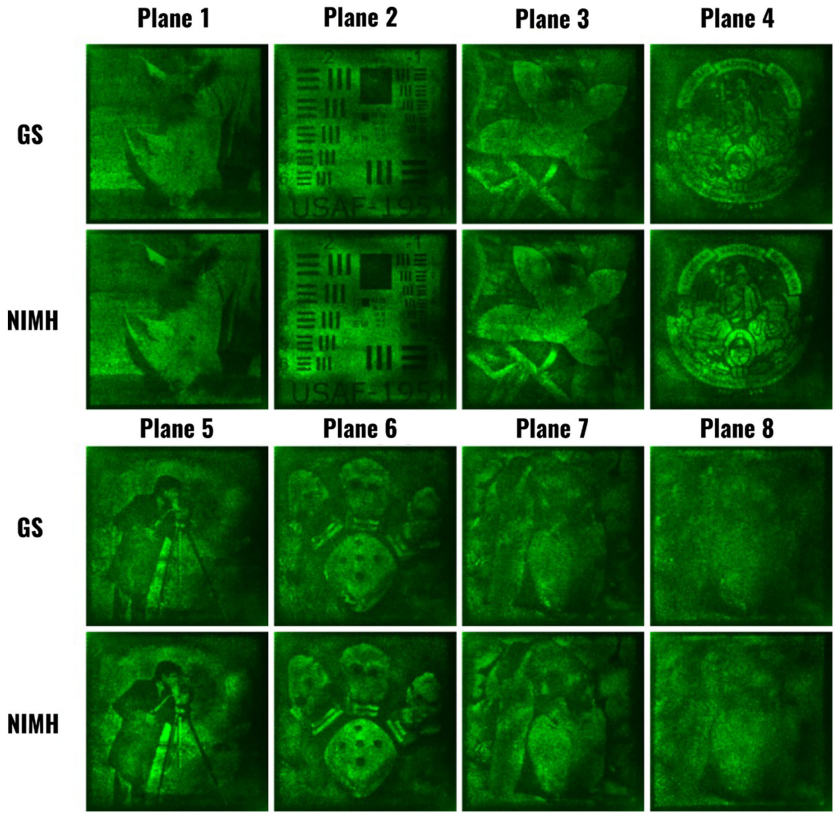

Fig. 10. Experimental comparison between the optical reconstruction of an eight-plane intensity distribution from a GS-generated hologram and a NIMH.

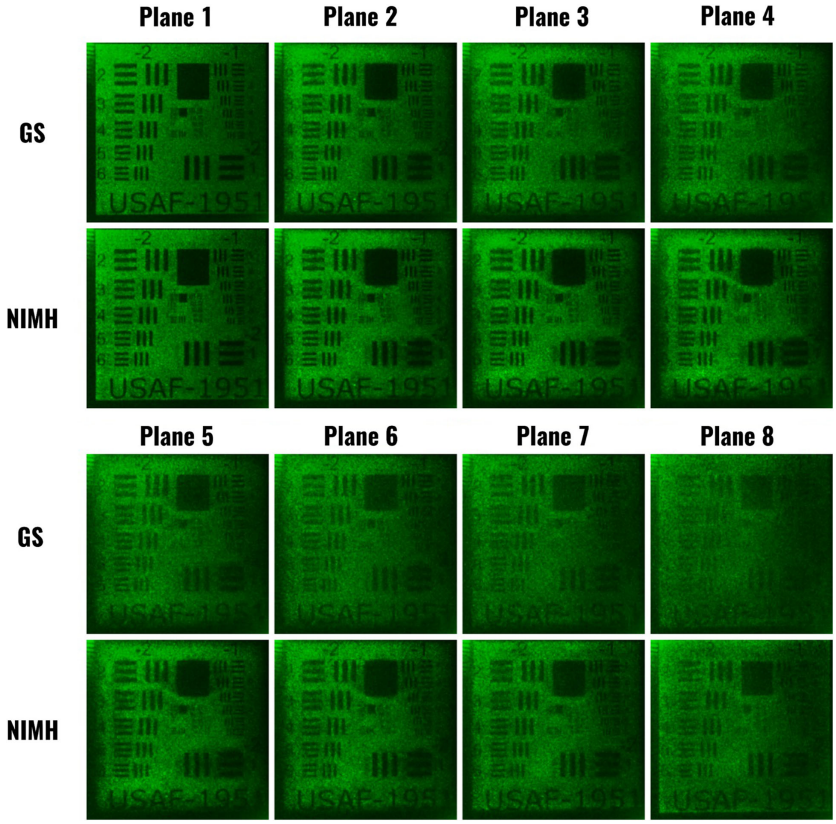

Fig. 11. Experimental comparison between the optical reconstruction of an eight-plane intensity distribution from a GS-generated hologram and a NIMH when using the same target in all planes.

the experiment shows a very similar performance to the numerical results of Fig. 5, despite the presence of additional sources of noise and the use of cut down holograms. In particular, we can see that the NIMH presents similar quality to the GS holograms in the first planes, and then better quality for the latter planes. This behavior is confirmed in the case where we use the same amplitude target in all planes, as shown in Fig. 11.

Again, the NIMH maintains similar quality to the GS holograms in the first planes and better quality in the latter planes. In particular, the difference in performance between both types of holograms is particularly noticeable in planes 7 and 8, where the GS hologram reconstruction is heavily affected by noise.

In Visualization 1, we include a video of the different reconstruction planes of the GS hologram for the test of Fig. 10. Each frame corresponds to a 0.08 cm displacement in the reconstruction distance. Visualization 2 contains the same video for the NIMH reconstructions. Visualization 3 shows the reconstruction of the GS hologram of the test of Fig. 11, while Visualization 4 is the reconstruction of the NIMH for that test. These videos highlight how, as the reconstruction distance is changed from plane to plane, the light remains confined in the same region of space. In this way, there is little loss of energy over all the intensity distribution. This is an important advantage of NIMH over using a superposition method.

5. CONCLUSIONS

The NIMH generation method shown in this paper allows the reproduction of complex, multiplane intensity distributions by using any kind of amplitude constraints. We demonstrated similar performance to the conventional multiplane GS algorithm for three-plane intensity distributions, and improved performance for eight-plane distributions. Furthermore, NIMH can be generated significantly faster than the GS holograms. Tests involving different interplane distances and experimental reconstructions are shown, validating our method. We believe that the NIMH can contribute to the development of novel applications, like multifocus head-up displays or holographic projection, while enabling faster dynamic optical trapping or neuronal photostimulation. Additionally, the NIMH could be combined with hybrid methods such as optimized random phases to achieve even greater fidelity after reconstruction. Moreover, a noniterative method to combine several amplitude constraints into a single hologram may be of use for holographic data compression, leading to new advancements in the field.

Funding. Consejo Nacional de Investigaciones Científicas y Técnicas (0849/16); Universidad Nacional de La Plata (11/I215).

Disclosures. The authors declare no conflicts of interest.

REFERENCES

1. A. Hussain, T. Amin, C. Kuang, L. Cao, and X. Liu, "Simple fringe illumination technique for optical superresolution," J. Opt. Soc. Am. B **34**, B78–B84 (2017).
2. A. Hussain, J. L. Martínez, A. Lizana, and J. Campos, "Super resolution imaging achieved by using on-axis interferometry based on a spatial light modulator," Opt. Express **21**, 9615–9623 (2013).
3. A. Velez-Zea, J. F. B. Ramírez, and R. Torroba, "Secure real-time generation and display of color holographic movies," Opt. Lasers Eng. **122**, 239–244 (2019).
4. A. Velez-Zea, J. F. Barrera Ramirez, and R. Torroba, "Optimized random phase encryption," Opt. Lett. **43**, 3558–3561 (2018).
5. H. Chen, Y. Guo, Z. Chen, J. Hao, J. Xu, H.-T. Wang, and J. Ding, "Holographic optical tweezers obtained by using the three-dimensional Gerchberg–Saxton algorithm," J. Opt. **15**, 035401 (2013).
6. H. Kim, M. Kim, W. Lee, and J. Ahn, "Gerchberg-Saxton algorithm for fast and efficient atom rearrangement in optical tweezer traps," Opt. Express **27**, 2184–2196 (2019).
7. F. Anselmi, C. Ventalon, A. Begue, D. Ogden, and V. Emiliani, "Three-dimensional imaging and photostimulation by remote-focusing and holographic light patterning," Proc. Natl. Acad. Sci. USA **108**, 19504–19509 (2011).
8. R. W. Gerchberg and W. O. Saxton, "A practical algorithm for the determination of phase from image and diffraction plane pictures," Optik **35**, 237–246 (1972).
9. M. Makowski, "Three-plane phase-only computer hologram generated with iterative Fresnel algorithm," Opt. Eng. **44**, 125805 (2006).
10. R. G. Dorsch, A. W. Lohmann, and S. Sinzinger, "Fresnel ping-pong algorithm for two-plane computer-generated hologram display," Appl. Opt. **33**, 869–875 (1994).
11. T. Harte, G. D. Bruce, J. Keeling, and D. Cassettari, "Conjugate gradient minimisation approach to generating holographic traps for ultracold atoms," Opt. Express **22**, 26548–26558 (2014).
12. J. Zhang, N. Pégard, J. Zhong, H. Adesnik, and L. Waller, "3D computer-generated holography by non-convex optimization," Optica **4**, 1306–1313 (2017).
13. H. Pang, J. Wang, A. Cao, and Q. Deng, "High-accuracy method for holographic image projection with suppressed speckle noise," Opt. Express **24**, 22766–22776 (2016).
14. D. Leseberg, "Computer-generated three-dimensional image holograms," Appl. Opt. **31**, 223–229 (1992).
15. C. K. Hsueh and A. A. Sawchuk, "Computer-generated double-phase holograms," Appl. Opt. **17**, 3874–3883 (1978).
16. V. Arrizón, "Improved double-phase computer-generated holograms implemented with phase-modulation devices," Opt. Lett. **27**, 595–597 (2007).
17. Y. K. Kim, J. S. Lee, and Y. H. Won, "Low-noise high-efficiency double-phase hologram by multiplying a weight factor," Opt. Lett. **44**, 3649–3652 (2019).
18. P. W. M. Tsang, Y. T. Chow, and T.-C. Poon, "Generation of patterned-phase-only holograms (PPOHs)," Opt. Express **25**, 9088–9093 (2017).
19. A. Velez-Zea, J. F. Barrera Ramirez, and R. Torroba, "Optimized random phase only holograms," Opt. Lett. **43**, 731–734 (2018).
20. A. Velez-Zea and R. Torroba, "Optimized random phase tiles for non-iterative hologram generation," Appl. Opt. **58**, 9013–9019 (2019).
21. R. Piestun, B. Spektor, and J. Shamir, "Wave fields in three dimensions: analysis and synthesis," J. Opt. Soc. Am. A **13**, 1837–1848 (1996).